SCIENCE CHINA PRESS

SCIENCE CHINA Life Sciences
life.scichina.com link.springer.com
https://doi.org/10.1007/s11427-023-2487-8

RESEARCH PAPER

The key role of myostatin b in somatic growth in fishes derived from distant hybridization

Qingfeng Liu[1,2], Lujiao Duan[1,2], Bei Li[1,2], Xuanyi Zhang[1,2], Fanglei Liu[1,2], Jianming Yu[1,2], Yuqin Shu[1,2], Fangzhou Hu[1,2], Jingjing Lin[2], Xiaoxia Xiong[2] & Shaojun Liu[1,2*]

[1]State Key Laboratory of Developmental Biology of Freshwater Fish, Hunan Normal University, Changsha 410081, China;
[2]College of Life Sciences, Hunan Normal University, Changsha 410081, China

*Corresponding author (email: lsj@hunnu.edu.cn)

Received 7 September 2023; Accepted 10 October 2023; Published online 29 March 2024

The basic mechanism of heterosis has not been systematically and completely characterized. In previous studies, we obtained three economically important fishes that exhibit rapid growth, WR (WCC ♀ × RCC ♂), WR-II (WR ♀ × WCC ♂), and WR-III (WR-II ♀ × 4nAU ♂), through distant hybridization. However, the mechanism underlying this rapid growth remains unclear. In this study, we found that WR, WR-II, and WR-III showed muscle hypertrophy and higher muscle protein and fat contents compared with their parent species (RCC and WCC). Candidate genes responsible for this rapid growth were then obtained through an analysis of 12 muscle transcriptomes. Notably, the mRNA level of *mstnb* (myostatin b), which is a negative regulator of myogenesis, was significantly reduced in WR, WR-II, and WR-III compared with the parent species. To verify the function of *mstnb*, a *mstnb*-deficient mutant RCC line was generated using the CRISPR-Cas9 technique. The average body weight of *mstnb*-deficient RCC at 12 months of age was significantly increased by 29.57% compared with that in wild-type siblings. Moreover, the area and number of muscle fibers were significantly increased in *mstnb*-deficient RCC, indicating hypertrophy and hyperplasia. Furthermore, the muscle protein and fat contents were significantly increased in *mstnb*-deficient RCC. The molecular regulatory mechanism of *mstnb* was then revealed by transcription profiling, which showed that genes related to myogenesis (*myod*, *myog*, and *myf5*), protein synthesis (PI3K-AKT-mTOR), and lipogenesis (*pparγ* and *fabp3*) were highly activated in hybrid fishes and *mstnb*-deficient RCC. This study revealed that low expression or deficiency of *mstnb* regulates somatic growth by promoting myogenesis, protein synthesis, and lipogenesis in hybrid fishes and *mstnb*-deficient RCC, which provides evidence for the molecular mechanism of heterosis via distant hybridization.

distant hybridization | heterosis | somatic growth | myostatin b | genome editing

INTRODUCTION

Distant hybridization is a classical breeding technique (Liu et al., 2020; Liu et al., 2022). Many fishes produced by distant hybridization have been widely used in aquaculture and have already generated substantial economic benefits (Gong et al., 2022; Hu et al., 2021). In China, among the 142 fishes that have been approved by the Ministry of Agriculture of China, 32 (22.53%) were derived from distant hybridization. In other countries, hybrid bass (Gaylord and Gatlin III, 2000), hybrid channel catfish (Argue et al., 2014), and hybrid tilapia (Wang et al., 2005; Xiao et al., 2022) have become economically important fishes. The offspring produced by distant hybridization usually exhibit multiple heteroses, such as rapid growth, a high survival rate, high stress resistance, high disease resistance, and high-quality meat (Liu, 2010). Although the molecular mechanisms underlying heterosis have always been a popular research topic, the basic mechanism of heterosis has not been systematically or completely elucidated. Many studies have suggested that heterosis is related to changes in gene structure (gene recombination and gene mutation) (Liu et al., 2018; Liu et al., 2016), gene expression (abnormal gene expression) (Li et al., 2018; Ren et al., 2019), and epigenetic modification (methylation and histone modification) (Ou et al., 2019; Ren et al., 2022), among other processes, caused by the fusion of two heterologous genomes (Ren et al., 2019). However, the molecular mechanisms of heterosis in distant hybrid fishes are largely unknown.

Fish muscle is not only a structural tissue and locomotive organ but also an important source of protein in human diets. From the perspective of breeding, fish breeders can promote the rapid development of muscle tissue by maximizing the promotion of muscle fibrocyte hyperplasia and hypertrophy to achieve rapid growth (Rescan, 2005; Rescan, 2008). Muscle fibers differentiate from somites under the action of myogenesis regulatory factors in fish (Johnston, 2006). The differentiation, proliferation, assembly, and regulation of muscle fibers together are the result of the expression of related functional genes and the interaction of regulatory factors during fish growth. The regulation of muscle mass and fiber size mainly reflects the changes in protein and fat contents, i.e., the balance of protein and fat synthesis and degradation within muscle fibers (Schiaffino et al., 2013). When muscle hypertrophy or hyperplasia occurs, protein and fat synthesis exceeds protein and fat degradation (Sartori et al., 2021).

Two major signaling pathways control muscle development and protein synthesis: the IGF1-AKT-mTOR pathway acts as a positive regulator, and the myostatin-Smad2/3 pathway acts as a negative regulator (Schiaffino et al., 2013; Shi et al., 2022; Xie et

al., 2018). Myostatin (*mstn*), which is also called growth differentiation factor 8, belongs to the TGF-β superfamily (Beyer et al., 2013). MSTN is a protein secreted mainly by skeletal muscle and plays a negative regulatory role in muscle development (Thomas et al., 2000). Mice with inactivated *mstn* show significant increases in muscle mass, gaining approximately 30% more weight than control mice (McPherron and Lee, 2002). Natural mutations in *mstn* are responsible for muscle growth in Belgian Blue and Piedmontese cattle with "double gluteal muscles" (McPherron and Lee, 1997). The structure of the *mstn* genes in fish is similar to that in mammals (Berry et al., 2002; Xu et al., 2003), and *mstn* genes are divided into two subtypes (*mstna* and *mstnb*), of which *mstnb* plays a more important role in postembryonic muscle growth (Kerr et al., 2005). Previous studies with some fishes have shown that *mstn* deletion causes hypertrophy and hyperplasia, resulting in significant increases in muscle mass (Chisada et al., 2011; Gao et al., 2016; Khalil et al., 2017; Kishimoto et al., 2018; Li et al., 2019; Tao et al., 2021; Wu et al., 2023; Zhong et al., 2016). Furthermore, as substantial body of evidence indicates that *mstn* plays a key role in lipid metabolism (Gao et al., 2016; McPherron and Lee, 2002; Tao et al., 2021).

We obtained three economically important fishes (WR, WR-II, and WR-III) by distant hybridization after more than 10 years of research. WR (2*n*=100) was obtained by the hybridization of female white crucian carp (*Carassius cuvieri*, WCC, 2*n*=100) and male red crucian carp (*Carassius auratus* red var., RCC, 2*n*=100) (Wang et al., 2015a), WR-II (2*n*=100) was obtained by the hybridization of female WR and male WCC (Liu et al., 2019a), and WR-III (3*n*=150) was obtained by the hybridization of female WR-II and male autotetraploid fish (4nAU, 4*n*=200) (Liu et al., 2021a) (Figure S1 in Supporting Information). WR, WR-II, and WR-III exhibit a more rapid growth rate than their parent species and have been farmed on a large scale in China, producing significant economic benefits. However, the basis of this rapid growth remains unclear. In this study, we found that WR, WR-II, and WR-III were hypertrophic compared with their parent species and exhibited higher muscle protein and fat contents. A subsequent muscle transcriptome analysis identified *mstnb* (myostatin b) as a candidate gene underlying their rapid growth. The *mstnb*-deficient mutant line of RCC was generated using the CRISPR-Cas9 technique. The body weight, the area and number of muscle fibers, and the protein and fat contents of muscle were significantly increased in *mstnb*-deficient RCC. Moreover, genes related to myogenesis (*myod*, *myog*, and *myf5*), protein synthesis (PI3K-AKT-mTOR), and lipogenesis (*pparγ* and *fabp3*) were found to be highly activated in hybrid fishes and *mstnb*-deficient RCC. In summary, we propose that *mstnb* plays a key role in the somatic growth of hybrid fishes by regulating myogenesis, protein synthesis, and lipogenesis. This study provides evidence of the molecular mechanism of heterosis produced by distant hybridization.

RESULTS

WR, WR-II, and WR-III show muscle fiber hypertrophy compared with the parent species

The appearances of RCC, WCC, WR, WR-II, and WR-III are shown in Figure 1A. Under the same conditions, the mean body weights of RCC, WCC, WR, WR-II, and WR-III at the age of one year were (252.6±10.6), (276.1±12.2), (303.7±16.7), (427.1±19.3) and (510.6±22.6) g, respectively. The mean body weights of WR, WR-II, and WR-III were significantly higher than those of their parent species (P<0.05). Significant differences in the average body weights were also detected among WR, WR-II, and WR-III (WR-III>WR-II>WR, P<0.05), and the average body weight of WCC was significantly higher than that of RCC (P<0.05). An analysis of the muscle fiber of RCC, WCC, WR, WR-II, and WR-III was conducted (Figure 1B–E). The mean fiber areas of WR ((3,350.3±193.2) μm^2), WR-II ((8,076±200.8) μm^2) and WR-III ((9,103±226.8) μm^2) were significantly higher than those of RCC ((2,665.1±130.3 μm^2) and WCC ((2,830.3±143.2) μm^2) (P<0.05) (Figure 1C); the total fiber areas of WR ((615,800±12,300) μm^2), WR-II ((626,809±13,210) μm^2) and WR-III ((710,343±15,289) μm^2) were significantly higher than those of RCC ((485,030±10,400) μm^2) and WCC ((537,700±11,090) μm^2) (P<0.05) (Figure 1E); the total fiber area of WCC was significantly higher than that of RCC (P<0.05) (Figure 1E); and the total numbers of fibers of WR-II (75.6±5.3) and WR-III (78.1±4.9) were significantly lower than those of RCC (182.5±6.7), WCC (190.3±9.6) and WR (188.2±7.2) (P<0.05) (Figure 1D). Furthermore, the results of the analysis of the nutritive composition showed that the muscle protein contents of WR, WR-II, and WR-III were higher than those of RCC and WCC (Figure S2A in Supporting Information), the muscle fat contents of WR and WR-II were higher than those of RCC and WCC (Figure S2B in Supporting Information), and the muscle fat content of WR-III was significantly higher than those of RCC and WCC (P<0.05) (Figure S2B in Supporting Information). In general, WR, WR-II, and WR-III showed rapid growth, muscle fiber hypertrophy, and higher protein and fat contents compared with RCC and WCC.

Identification of candidate genes for rapid growth by transcriptome analysis

To identify candidate genes for rapid growth (hypertrophy), a muscle transcriptome analysis of one-year-old RCC, WR, WR-II, and WR-III was performed. We obtained 5.04×10^8 (75.69 GB) clean reads from 12 muscle transcriptomes. The basic information of the transcriptome assembly is shown in Table S1 in Supporting Information, and the high repeatability between different samples from the same fish is shown in Figure S3 in Supporting Information. Using strict criteria, we found 4,080 differentially expressed genes (DEGs; upregulated: 1,934, downregulated: 2,146) between RCC and WR (Figure 2A and D), 5,573 DEGs (upregulated: 2,691, downregulated: 2,882) between RCC and WR-II (Figure 2B and E), and 5,904 DEGs (upregulated: 2,817, downregulated: 3,087) between RCC and WR-III (Figure 2C and F). The genes associated with growth were verified through GO and KEGG analyses and included genes annotated with the terms growth (GO:0040007), response to growth factor (GO:0070848), insulin-like growth factor binding (GO:0005520), insulin signaling pathway (ko04910), TGF-beta signaling pathway (ko04350), mTOR signaling pathway (ko04150) and FoxO signaling pathway (ko04068) (Tables S2–S4 in Supporting Information). The top 10 growth-related DEGs (*mstnb*, *fgf21* (fibroblast growth factor 21), *igf1r* (insulin-like growth factor 1), *htra1* (high-temperature requirement A serine peptidase 1), *igfbp7* (insulin-like growth factor-binding protein 7), *fgf12* (fibroblast growth factor 12), *pi3k* (phosphoi-

https://doi.org/10.1007/s11427-023-2487-8

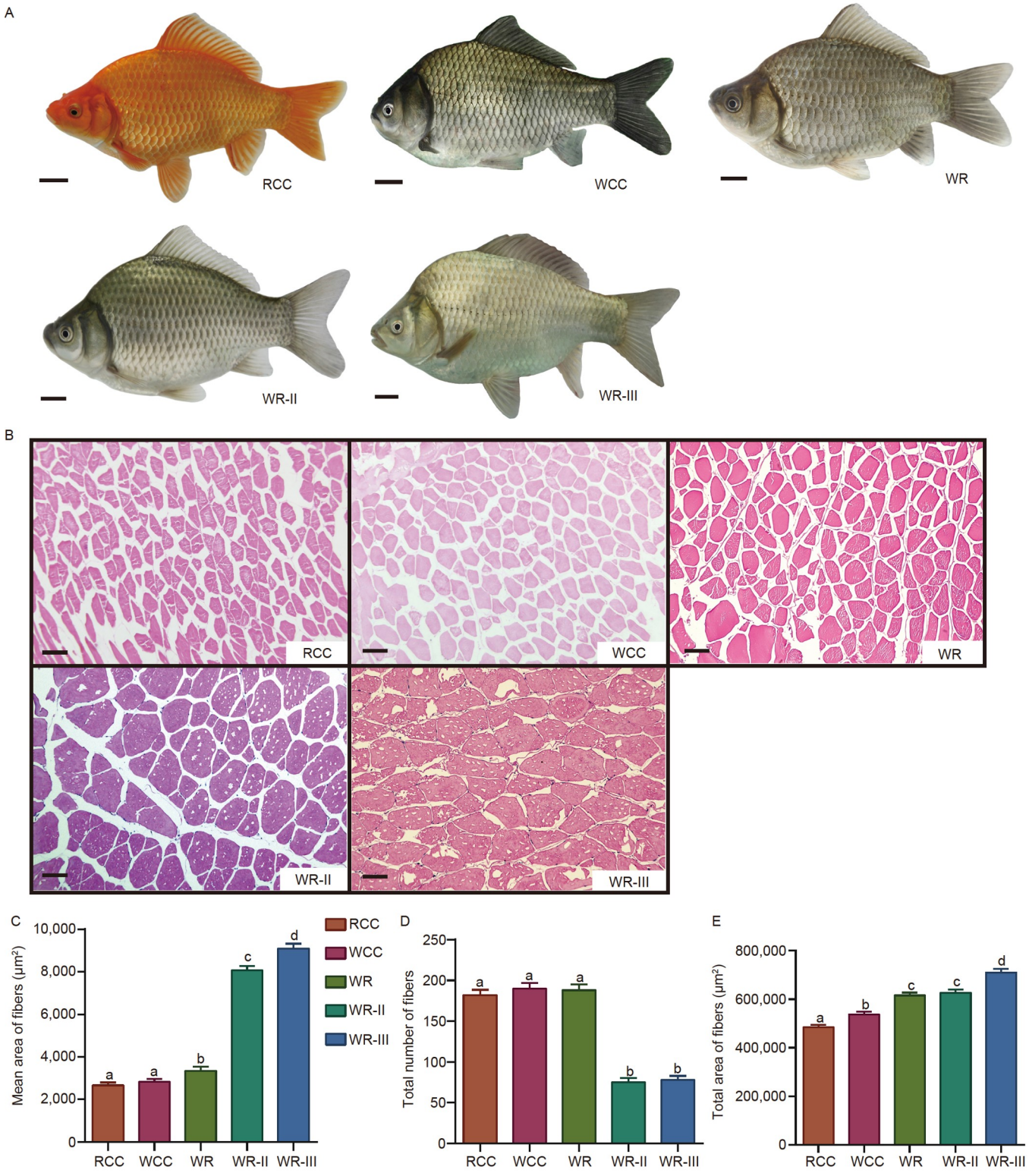

Figure 1. Hybrid fishes show muscle fiber hypertrophy compared with RCC and WCC. A, Appearances of RCC, WCC, WR, WR-II, and WR-III. Bar=2 cm. B, Paraffin sectioning and H&E staining of 12-month-old RCC, WCC, WR, WR-II, and WR-III. Representative pictures are shown. Bar=100 μm. C and D, Quantitative analyses of muscle fibers, including calculation of the mean fiber area (C), the total number of fibers (D), and the total fiber area (E), was performed by using ImageJ. Different lowercase letters indicate significant differences ($P<0.05$).

nositide 3-kinase), *cyr61* (cysteine-rich angiogenic inducer 61), *vegfa* (vascular endothelial growth factor a), and *akt* (protein kinase B)) shared by WR, WR-II, and WR-III were considered candidate genes for rapid growth (Table 1). A RT-qPCR of the candidate genes in RCC, WCC, WR, WR-II, and WR-III was then performed (Figure 3). Notably, the mRNA level of *mstnb*, which is

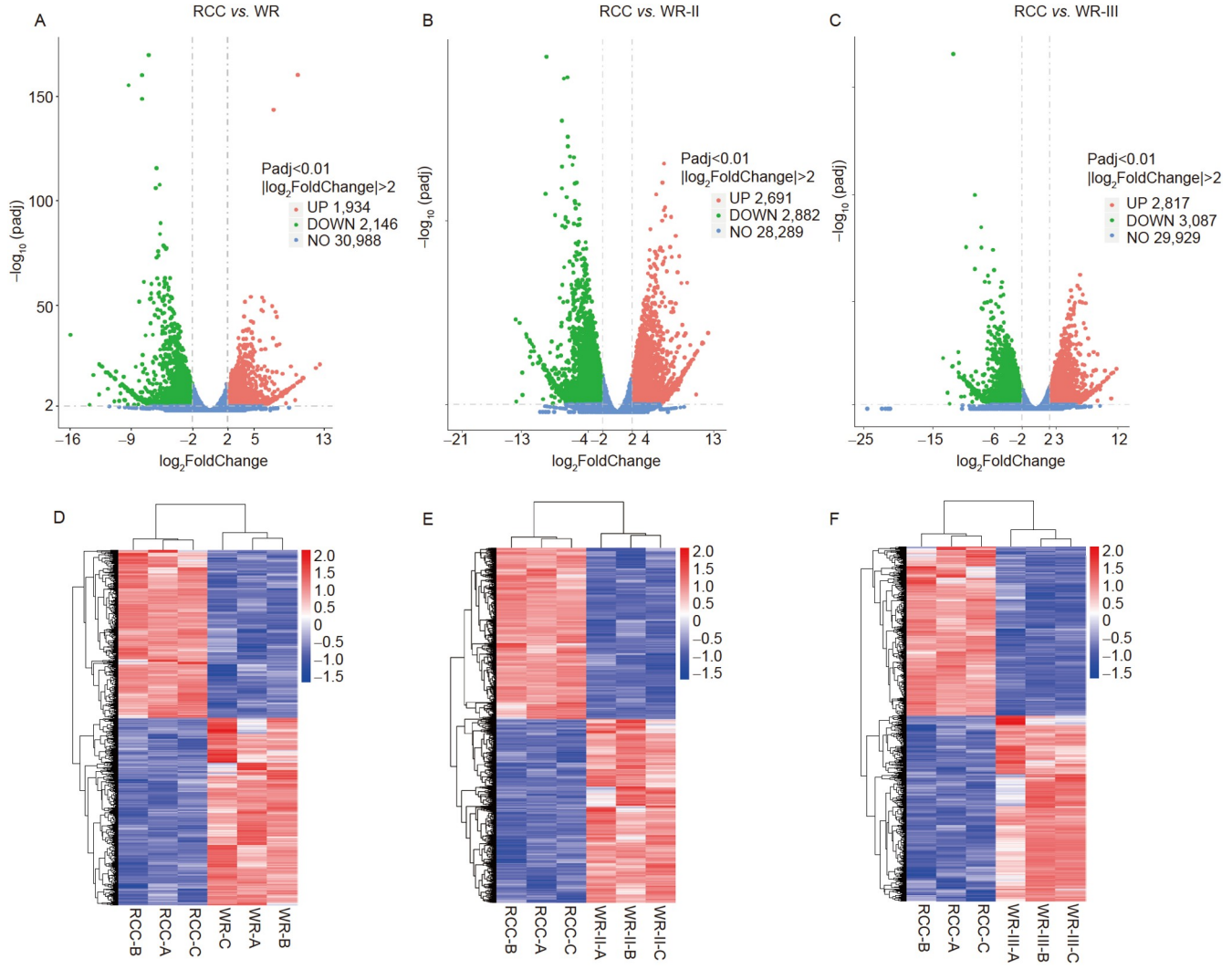

Figure 2. Identification of DEGs and clustering analysis of DEGs. A–C, Identification of DEGs in the RCC *vs.* WR (A), RCC *vs.* WR-II (B), and RCC *vs.* WR-III (C) comparisons. The criteria for DEGs were padj<0.01 and $|\log_2 \text{fold change}|>2$. D–F, Detailed hierarchical clustering of DEGs, including those identified from the RCC *vs.* WR (D), RCC *vs.* WR-II (E), and RCC *vs.* WR-III (F) comparisons. The colors and numbers indicate the changes in expression levels.

a negative regulator of myogenesis, was significantly lower in WR, WR-II, and WR-III than in RCC and WCC.

Generation of the RCC *mstnb*-depletion line

Based on the *mstnb*-coding DNA sequence (CDS) of RCC, we obtained the full-length *mstnb* CDSs of WR (WR-1 and WR-2), WR-II (WR-II-1 and WR-II-2), WR-III (WR-III-1, WR-III-2, and WR-III-3), and WCC by PCR (Figure S4 in Supporting Information). A sequence analysis revealed the following: the identity of the *mstnb* sequences of WR and RCC was 96.45% (WR-1) and 99.47% (WR-2), the identity of the *mstnb* sequences of WR-II and RCC was 96.63% (WR-II-1) and 99.47% (WR-II-2), the identity of the *mstnb* sequences of WR-III and RCC was 96.45% (WR-III-1), 99.02% (WR-III-2) and 98.85% (WR-III-3), the identity of the *mstnb* sequences of WCC and RCC was 96.45%, the identity of the *mstnb* sequences of WR and zebrafish was 93.71% (WR-1) and 92.29% (WR-2), the identity of the *mstnb* sequences of WR-II and zebrafish was 93.88% (WR-II-1) and 92.73% (WR-II-2), the identity of the *mstnb* sequences of WR-III and zebrafish was 93.35% (WR-III-1), 92.20% (WR-III-2), and 92.73% (WR-III-3), and the identity of the *mstnb* sequences of WCC and zebrafish was 93.71%. These results indicated that the function of *mstnb* in these fishes is highly conserved. To verify the effect of *mstnb* on rapid growth (hypertrophy), we obtained an *mstnb*-deficient mutant line

Table 1. Genes associated with growth shared among the sets of WR, WR-II, and WR-III DEGs

Gene symbol	$\log_2$(RCC/WR)	$\log_2$(RCC/WR-II)	$\log_2$(RCC/WR-III)
mstnb	2.05	3.62	2.61
fgf21	2.81	5.06	4.96
igf1r	−5.38	−4.39	−3.07
htra1	−4.45	−8.05	−5.98
igfbp7	−4.30	−5.76	−4.42
fgf12	−3.41	−5.63	−3.34
pi3k	−4.00	−5.92	−4.50
cyr61	−2.92	−5.72	−5.10
vegfa	−2.11	−2.12	−3.57
akt	−2.01	−2.35	−2.77

https://doi.org/10.1007/s11427-023-2487-8

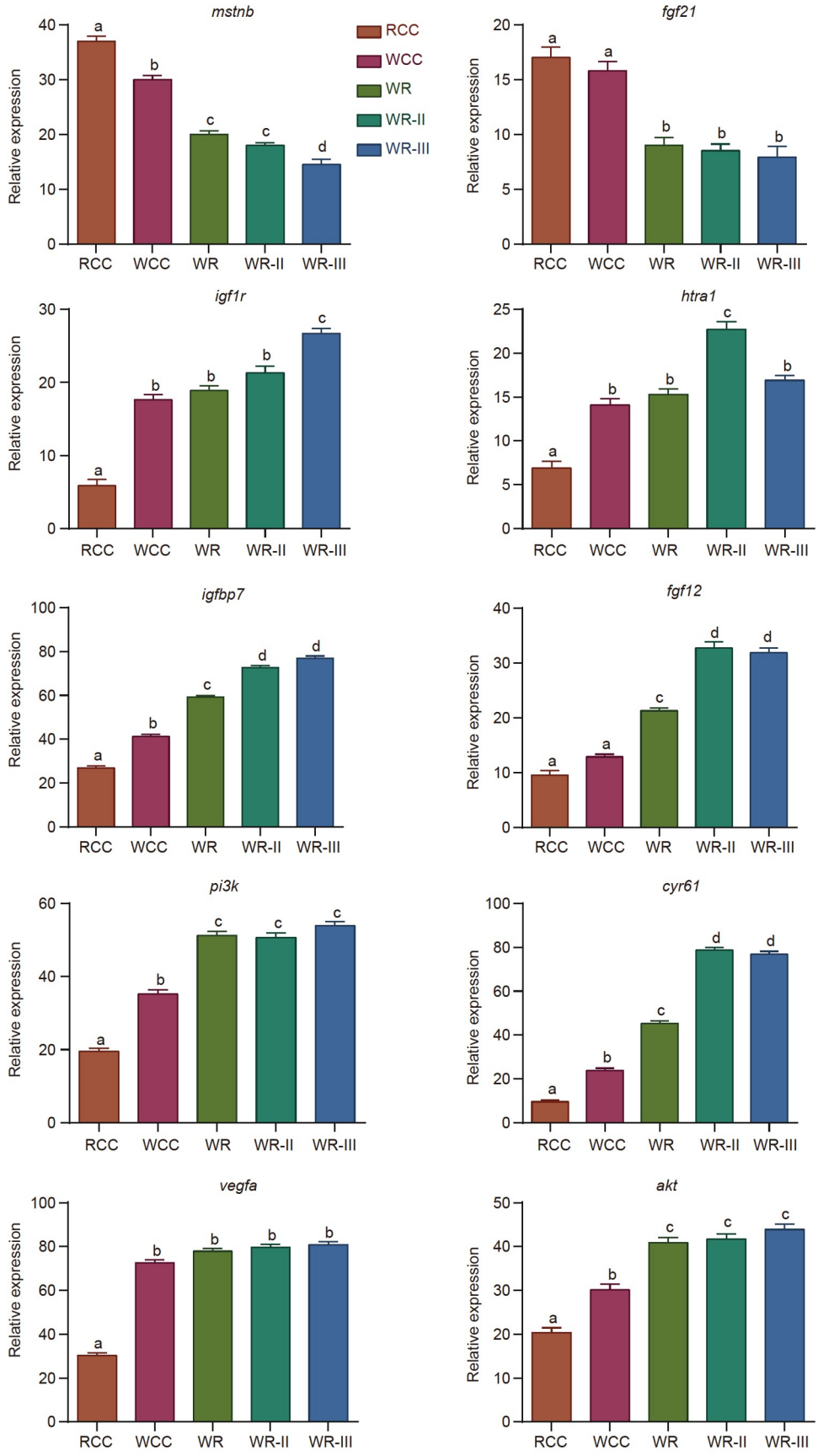

Figure 3. The relative mRNA levels of growth candidate genes in RCC, WCC, WR, WR-II, and WR-III were determined by RT-qPCR. Different lowercase letters indicate significant differences ($P<0.05$).

of RCC using the CRISPR-Cas9 technique. The F_0 mutant was produced by injecting a mixture of Cas9 mRNA and *mstnb* gRNA into the embryos, and the resulting gene disruption was confirmed by PCR. The F_1 heterozygote was produced by the mating of F_0 and wild-type RCC, and the PCR products of F_1 showed multiple peaks compared with those obtained with wild-type RCC (Figure S5A and B in Supporting Information). The F_2 homozygote (*mstnb*-deficient RCC) was obtained by self-crossing F_1. The PCR products obtained from F_2 fish are shown in Figure S5C in Supporting Information, and the genotypes were confirmed by PCR (Figure 4A). The *mstnb*-deficient RCC line was established by self-crossing F_2. The RT-qPCR results showed that the *mstnb* mRNA level was significantly reduced in *mstnb*-deficient RCC compared with that in wild-type RCC ($P<0.05$) (Figure 4B). Furthermore, the *mstnb* protein level of *mstnb*-deficient RCC was significantly lower than that of wild-type RCC ($P<0.05$) (Figure 4C).

mstnb-deficient RCC exhibit a greater body weight and enhanced muscle fiber hypertrophy and hyperplasia

The body weights of *mstnb*-deficient RCC and wild-type RCC reared under the same conditions were measured. The results showed that the average body weight of *mstnb*-deficient RCC was significantly higher than that of wild-type RCC beginning at 3 months of age, and the body weight of *mstnb*-deficient RCC ((261.6±11.2) g) was 29.57% greater than that of wild-type RCC at 12 months of age ((201.9±9.7) g) (Figure 5A and B). Furthermore, a muscle fiber analysis showed that *mstnb*-deficient RCC had characteristics of muscle fiber hypertrophy and hyperplasia compared with wild-type RCC (Figure 5C). The total number of fibers in *mstnb*-deficient RCC (221±6.6) was significantly higher than that in wild-type RCC (193±5.1) ($P<0.05$) (Figure 5D), the mean fiber area of *mstnb*-deficient RCC ((1,969.1±75.9) μm^2) was significantly higher than that of wild-type RCC ((1,580.6±70.3) μm^2) ($P<0.05$) (Figure 5E), and the total fiber area of *mstnb*-deficient RCC ((431,089±19,453) μm^2) was significantly higher than that of wild-type RCC ((302,658±17,000) μm^2) ($P<0.05$) (Figure 5F).

Depletion of *mstnb* promotes protein synthesis and adipogenesis in RCC

The analysis of muscle nutrients showed that the protein and fat contents of *mstnb*-deficient RCC ((16.8±0.34) g/100 g, (2.7±0.08) g/100 g)) were significantly higher than those of wild-type RCC ((15.3±0.22) g/100 g, (1.4±0.05) g/100 g) ($P<0.05$) (Figure 6A and B)), and the amino acid, flavored amino acid, moisture and ash contents of *mstnb*-deficient RCC were not significantly different from those of wild-type RCC ($P>0.05$) (Figure 6C–F). The results indicated that depletion of *mstnb* promotes protein synthesis and adipogenesis.

Depletion of *mstnb* stimulates the expression of myogenesis-, protein metabolism-, and lipid metabolism-related genes

To explore the molecular mechanism by which *mstnb* deficiency promotes hypertrophy, hyperplasia, protein synthesis, and adipogenesis, the transcription levels of genes related to

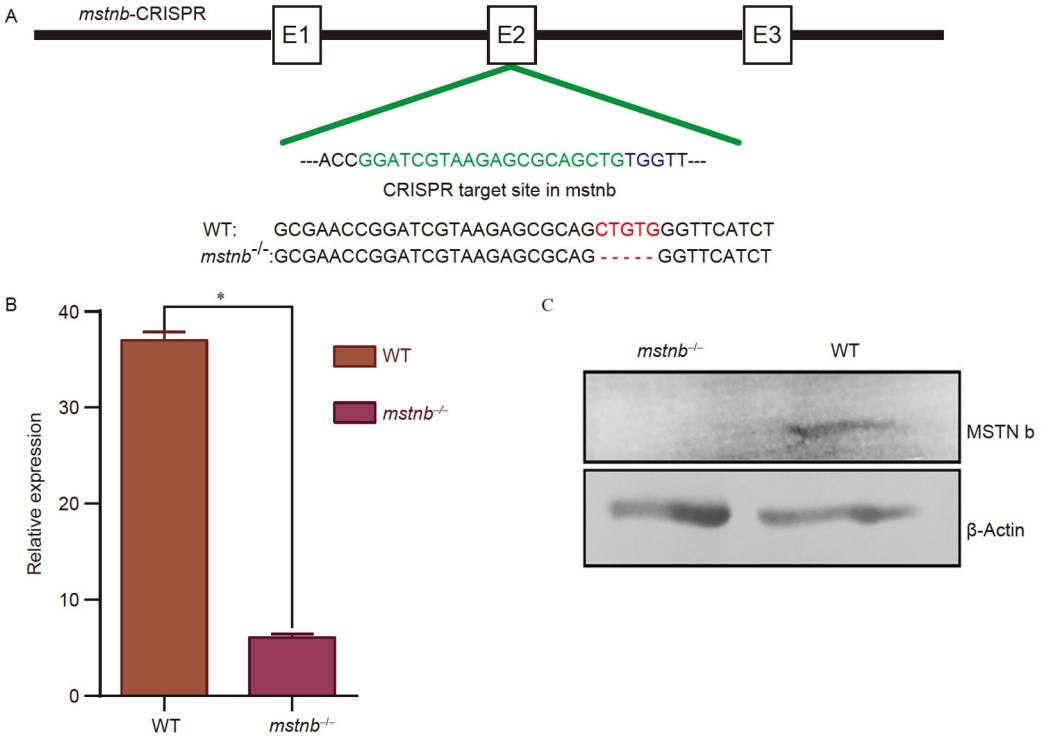

Figure 4. The *mstnb*-deficient mutant line in RCC was generated using CRISPR-Cas9. A, Schematic of the CRISPR target site in the *mstnb* gene and sequence of the *mstnb* mutation. The target site is marked in green, and the PAM sequence is labeled in blue. E, exon. The deleted bases are shown as red dashes. B, Fold change in *mstnb* mRNA levels in *mstnb*$^{-/-}$ RCC and wild-type siblings. * indicates a significant difference ($P<0.05$). C, Western blotting of *mstnb* in muscle of *mstnb*$^{-/-}$ RCC and wild-type siblings. β-Actin was used as a control.

https://doi.org/10.1007/s11427-023-2487-8

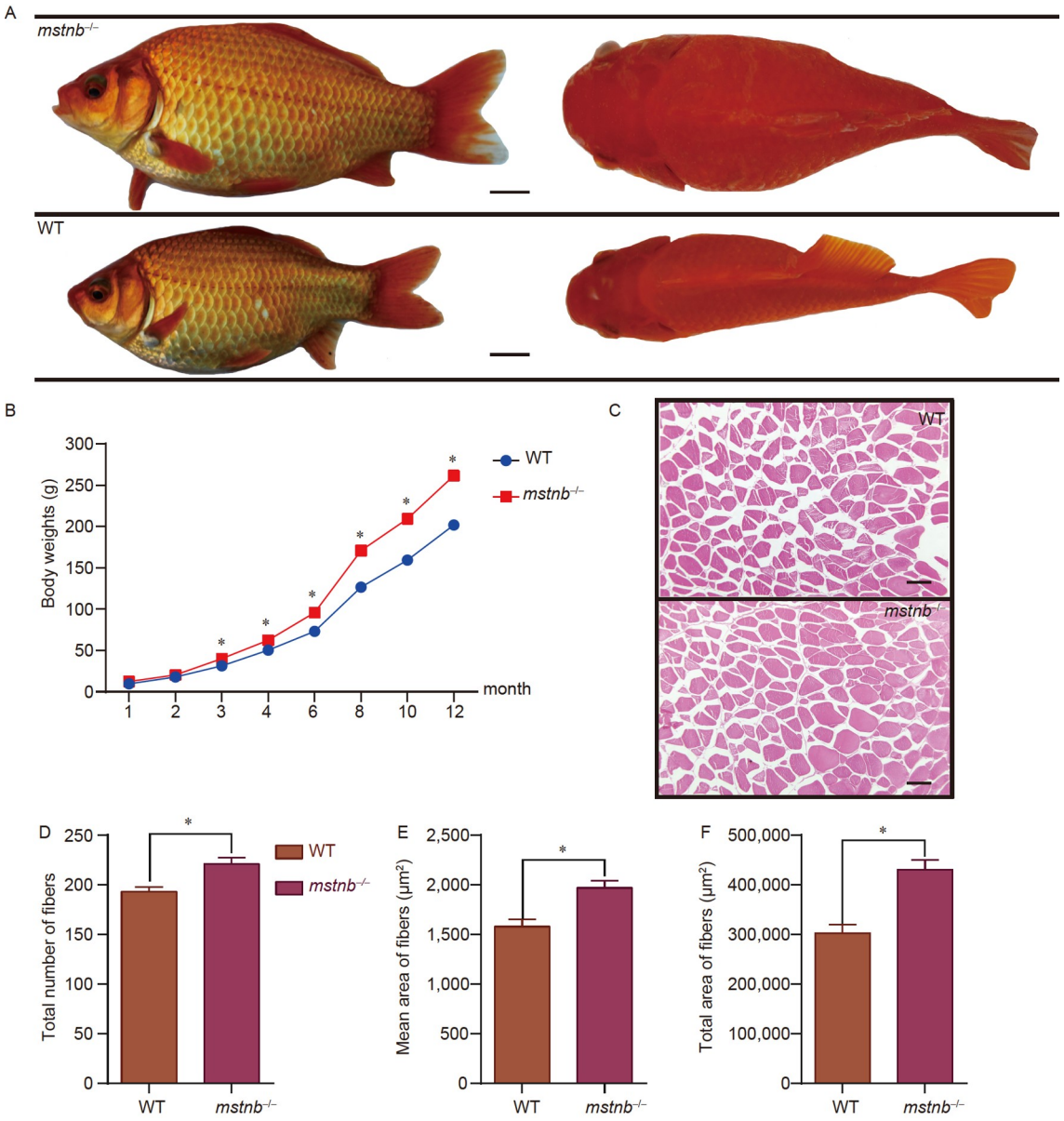

Figure 5. Depletion of *mstnb* promotes growth and muscle fiber hypertrophy and hyperplasia in RCC. A, Appearances of *mstnb*$^{-/-}$ RCC and wild-type siblings. Bar=2 cm. B, Average body weights of *mstnb*$^{-/-}$ RCC and wild-type siblings from 1 to 12 months of age. C, Paraffin sectioning and H&E staining of 12-month-old *mstnb*$^{-/-}$ RCC and wild-type siblings. Representative images are displayed. Bar=100 μm. D–F, Quantitative analyses of muscle fibers, including calculation of the total number of fibers (D), the mean fiber area (E), and the total fiber area (F), were performed using ImageJ. * indicates a significant difference (P<0.05).

myogenesis, protein metabolism, lipid metabolism, and growth at the age of one year were detected by RT-qPCR. Among myogenesis-related genes, the mRNA levels of *myod* (myogenic differentiation antigen), *myog* (myogenin), and *myf*5 (myogenic factor 5) were significantly increased in *mstnb*-deficient RCC compared with wild-type RCC (Figure 7A). Among protein metabolism-related genes, the mRNA levels of *akt*, *mtor* (mechanistic target of rapamycin), *pi3k*, *rps6* (ribosomal protein S6), *rps6kb* (ribosomal protein S6 kinases), *foxo1* (forkhead box O1), and *foxo3* (forkhead box O3) were significantly increased in *mstnb*-deficient RCC compared with wild-type RCC (Figure 7B). In particular, the mRNA levels of *pi3k* and *akt* (protein synthesis-related genes) were increased 2.7-fold in *mstnb*-deficient RCC compared with wild-type RCC. In addition, the mRNA levels of *4ebp1* (eukaryotic translation initiation factor 4E-binding protein 1), *erk1* (extracellular regulated protein kinase), and *foxo4* (forkhead box O4) (protein metabolism-related genes) displayed no significant difference between *mstnb*-deficient RCC and wild-type RCC (Figure 7B).

Among lipid metabolism-related genes, the mRNA levels of *fadd* (Fas-associated protein with death domain), *pparγ* (peroxisome proliferator-activated receptor γ), *pparβ* (peroxisome proliferator-activated receptor β), *pparα* (peroxisome proliferator-activated receptor α), *lxrα* (liver X receptor α), *fabp3* (fatty acid binding protein 3), *ucp2* (uncoupling protein 2) and *lipe* (hormone-sensitive lipase) were significantly increased in *mstnb*-deficient RCC compared with wild-type RCC (Figure 7C). In particular, the mRNA levels of *pparγ* and *fabp3* (adipogenesis-related genes) were

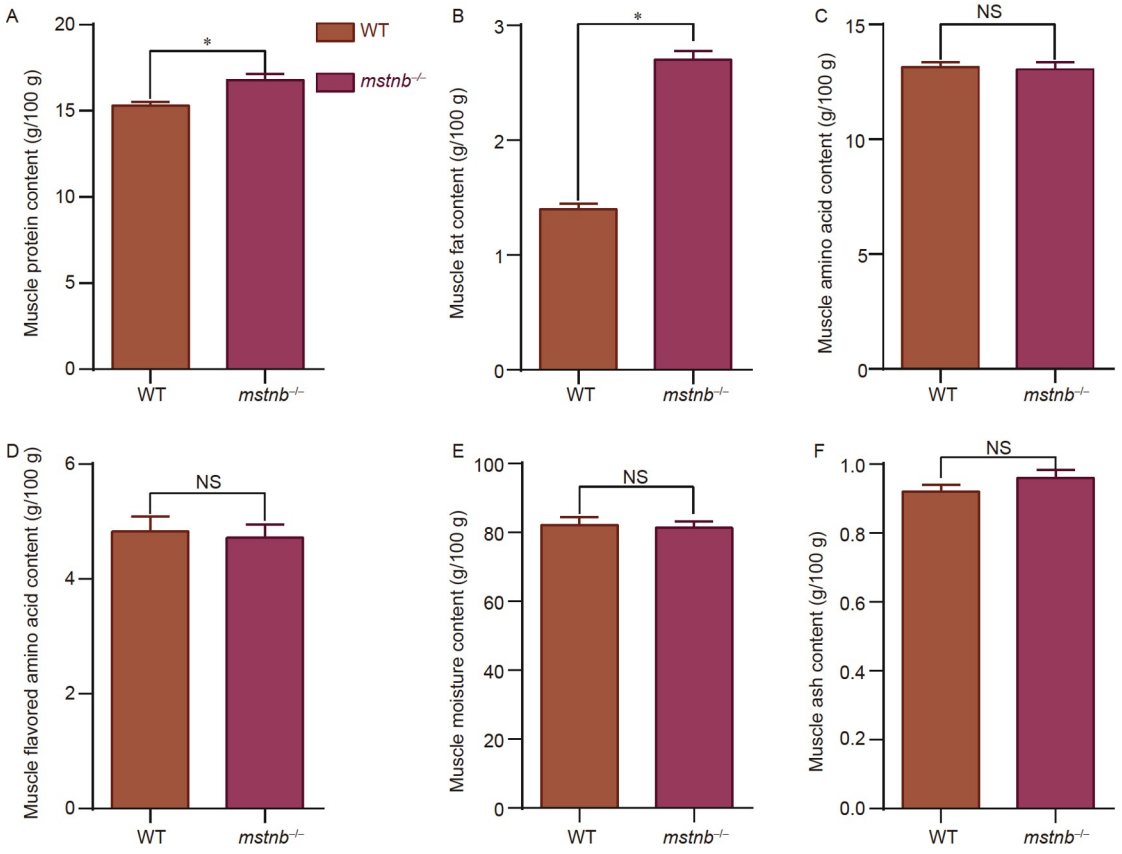

Figure 6. Muscle nutrient analysis of *mstnb*$^{-/-}$ RCC and wild-type siblings. A, Muscle protein content. B, Muscle fat content. C, Muscle amino acid content. D, Muscle flavored amino acid content. E, Muscle moisture content. F, Muscle ash content. * indicates a significant difference (P<0.05), and NS indicates no significant difference (P>0.05).

increased 2.1-fold in *mstnb*-deficient RCC compared with wild-type RCC. The mRNA levels of *fgf21*, *igf1r*, *htra1*, *igfbp7*, *cyr61*, *vegfa*, and *acvr2b* (activin a receptor type 2b) (rapid growth candidate genes) were significantly increased in *mstnb*-deficient RCC compared with wild-type RCC (Figure 7D). The mRNA levels of the lipid metabolism-related genes *lpl* (lipoprotein lipase) and *fas* (Fas cell surface death receptor) and the growth-related gene *fgf12* displayed no significant difference between *mstnb*-deficient RCC and wild-type RCC (Figure 7C and D).

The mRNA expression of myogenesis-, protein metabolism-, and lipid metabolism-related genes is significantly increased in hybrid fishes compared with their parent species

Based on the expression of myogenesis-, lipid-, and protein metabolism-related genes in *mstnb*-deficient RCC and wild-type RCC, the expression patterns of these genes in the hybrid fishes (WR, WR-II, WR-III) and parent species (RCC and WCC) were determined (Figures 3 and 8). Among the myogenesis-related genes, the mRNA levels of *myog* were significantly increased in WR, WR-II, and WR-III compared with RCC and WCC, and the mRNA levels of *myod* were significantly higher in WR-II and WR-III than in RCC and WCC, whereas the mRNA levels of *myf5* displayed no significant difference among WR, WR-II, WR-III, RCC, and WCC. Among the protein metabolism-related genes, the mRNA levels of *akt*, *mtor*, *pi3k*, *rps6*, and *foxo3* were significantly increased in WR, WR-II, and WR-III compared with RCC and WCC; the mRNA level of *foxo1* was significantly increased in WR, WR-II, and WR-III compared with RCC; and the mRNA level of *rps6kb* was significantly increased in WR-II and WR-III compared with RCC and WCC. Among the lipid metabolism-related genes, the mRNA levels of *pparγ* and *fabp3* were significantly increased in WR, WR-II, and WR-III compared with RCC and WCC; the mRNA levels of *fadd*, *ucp2*, and *lipe* were significantly increased in WR, WR-II, and WR-III compared with RCC; the mRNA levels of *pparβ* and *pparα* were significantly increased in WR-II and WR-III compared with RCC and WCC; and the mRNA level of *lxrα* was significantly increased in WR-III compared with RCC and WCC. In general, genes related to myogenesis, protein metabolism, and lipid metabolism were activated in hybrid fishes.

DISCUSSION

Distant hybridization is a classical and widely used technique, and heterosis has been extensively exploited in fisheries (Bartley et al., 2000; Li et al., 2022; Liu et al., 2021b). In previous studies, we obtained three economically important fishes, WR, WR-II, and WR-III, by distant hybridization (Liu et al., 2019a; Liu et al., 2021a; Liu et al., 2019b; Wang et al., 2015a). These hybrid fishes have the advantage of rapid growth and are cultivated on a large scale in China, but the mechanism of their rapid growth remains a mystery. In fish, the muscle weight accounts for most of the body weight, and rapid growth is mainly due to the rapid development of muscle fibrocytes. In this study, we found that the

https://doi.org/10.1007/s11427-023-2487-8

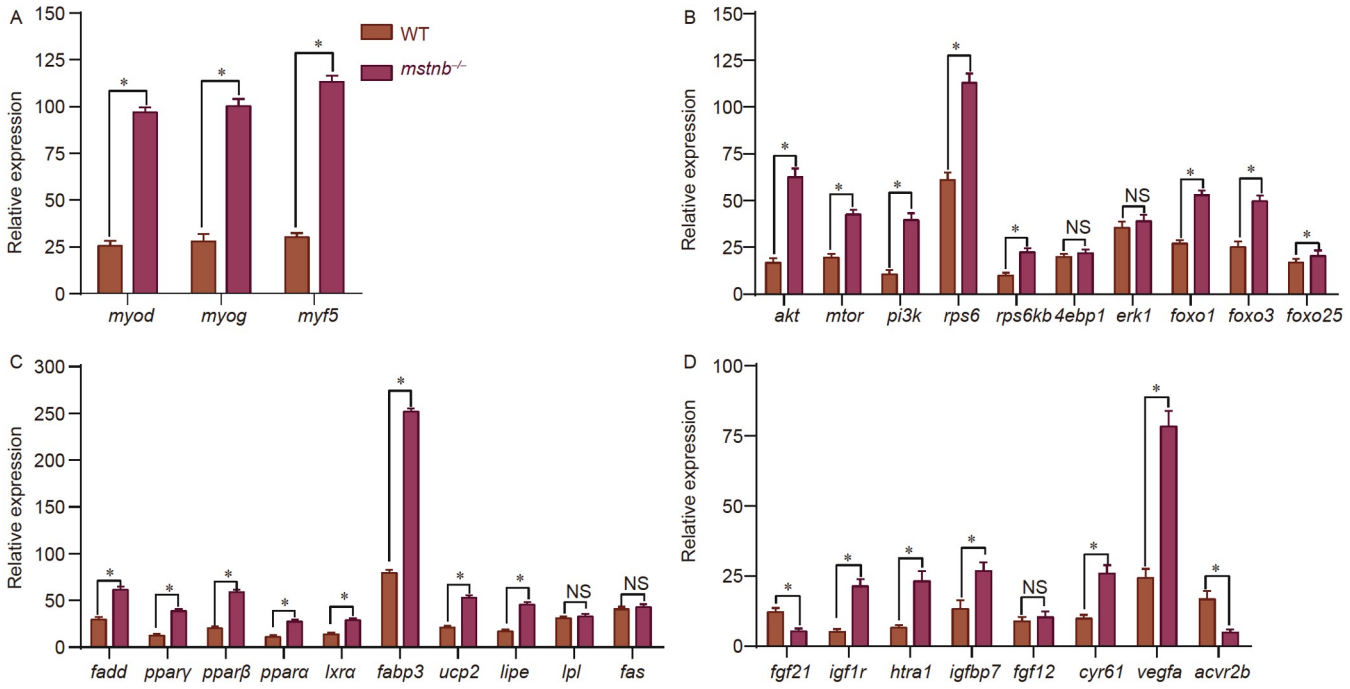

Figure 7. The relative mRNA levels of key myogenesis-, protein metabolism-, lipid metabolism-, and growth-related genes in *mstnb*$^{-/-}$ RCC and wild-type siblings were determined by RT-qPCR. A, Myogenesis-related genes. B, Metabolism-related genes. C, Lipid metabolism-related genes. D, Growth-related genes. * indicates a significant difference (P<0.05), and NS indicates no significant difference (P>0.05).

mean area and total area of muscle fibers in WR, WR-II, and WR-III were significantly higher than those in the parent species (RCC and WCC), indicating muscle fiber hypertrophy (Figure 1B–E). This result provides direct cell-level evidence showing that the rapid growth of these hybrid fishes might be caused by muscle fiber hypertrophy. Furthermore, we found that the protein and fat contents of WR, WR-II, and WR-III were higher than those of RCC and WCC (Figure S2 in Supporting Information). To reveal the molecular mechanism of rapid growth (hypertrophy), the muscle transcriptomes from 12 WR, WR-II, WR-III, and RCC samples were analyzed (Figure 2). Interestingly, many signaling pathways and key genes were shared among the DEGs identified from the comparisons of WR, WR-II, and WR-III with RCC (Tables S2–S4 in Supporting Information). This finding might be due to the special genetic relationship among these fishes (Figure S1 in Supporting Information) and might also indicate that the molecular mechanism of rapid growth may be similar among them. Moreover, 10 genes shared by WR, WR-II, and WR-III were selected as candidate genes for rapid growth through bioinformatics analysis (Table 1 and Figure 3). Notably, the mRNA level of *mstnb*, which is a negative regulator of myogenesis, was significantly reduced in WR, WR-II, and WR-III compared with RCC and WCC (Figure 3). MSTN is a protein secreted mainly by skeletal muscle, and loss of *MSTN* function can promote rapid muscle growth (Lee et al., 2020). In cattle, mice, goats, zebrafish, common carp, Nile tilapia, loach, red sea bream, channel catfish, and medaka, *mstn* mutants show muscle hypertrophy and/or muscle hyperplasia, as revealed in previous studies (Gao et al., 2016; Kambadur et al., 1997; Khalil et al., 2017; Kishimoto et al., 2018; Lee et al., 2012; Tao et al., 2021; Whittemore et al., 2003; Wu et al., 2023; Yeh et al., 2017; Yu et al., 2016; Zhong et al., 2016). Furthermore, we found that the *mstnb* CDS regions of WR, WR-II, WR-III, RCC, WCC, and zebrafish were highly similar (>92%, Figure S3 in Supporting Information), indicating that they have similar functions. Based on the mRNA expression profile of *mstnb* in hybrid fishes, the high conservation of *mstnb* CDS in hybrid fishes, and the existing relevant reports on the function of *mstnb*, we speculated that the low expression of *mstnb* may be one of the key reasons for the rapid growth (hypertrophy) of hybrid fishes.

To verify the function of *mstnb* in hybrid fishes and RCC, an *mstnb*-deficient mutant RCC line was established using the CRISPR-Cas9 technique (Figures 4 and 5A). We found that the average weight of one-year-old *mstnb*-deficient RCC was significantly higher (29.57%) than that of age-matched wild-type RCC (Figure 5B). As observed in previous studies, mutations of *mstn* increase the body weight of mammals by 15%–30% (Crispo et al., 2015; Guo et al., 2016; Lee et al., 2012; Wang et al., 2015b) and that of zebrafish, medaka, red sea bream, channel catfish, loach, and Nile tilapia by 10%–49% (Chisada et al., 2011; Gao et al., 2016; Khalil et al., 2017; Kishimoto et al., 2018; Tao et al., 2021; Wu et al., 2023), consistent with the results found for RCC in this study. However, *mstnb*-deficient RCC showed significant growth differences at the juvenile stage (age of 3 months) (Figure 5B), *mstnb*-deficient zebrafish exhibit showed growth differences in adulthood (80 days postfertilization) (Gao et al., 2016), *mstn*-deficient medaka show growth differences at the post-juvenile stage (3 weeks post-hatching) (Chisada et al., 2011), and *mstn*-deficient loach show growth differences at the juvenile stage (1 month of age) (Tao et al., 2021). These findings indicated that *mstn* begins to inhibit muscle growth at different time points in different fishes. Furthermore, we found that the total number and total area of fibers in *mstnb*-deficient RCC were significantly higher than those in wild-type RCC, demonstrating muscle hypertrophy and muscle hyperplasia (Figure 5C–F). This finding is consistent with reports about the effect of *mstn* on

myogenesis in medaka and loach (Chisada et al., 2011; Tao et al., 2021), indicating the conserved function of *mstn*. These findings were consistent with the characteristics of muscle hypertrophy in one-year-old WR, WR-II, and WR-III compared with RCC and WCC (Figure 1B–E), indicating that low expression of *mstnb* promotes muscle hypertrophy in hybrid fishes. The regulation of muscle mass and muscle fiber size mainly reflects changes in the protein and fat contents. In mammals, *mstn* plays an important role in protein synthesis and adipogenesis (Deng et al., 2017; McPherron and Lee, 2002; Schiaffino et al., 2013; Shan et al., 2013). Purified myostatin is capable of inhibiting protein synthesis in C_2C_{12} muscle cells (Taylor et al., 2001). In mice, mutation of *mstn* promotes the burning of white adipose tissue (WAT), and the body fat mass is significantly reduced in these animals (Shan et al., 2013). However, in fish, *mstn* exerts both positive and negative regulatory effects on muscle fat (Gao et al., 2016; Li et al., 2019; Tao et al., 2021), and the effect of *mstn* on protein synthesis has rarely been investigated. In this study, we found that both the protein and fat contents were significantly increased in *mstnb*-deficient RCC (Figure 6A and B), which indicates that *mstnb* negatively regulates the synthesis of muscle protein and muscle fat in RCC. This conclusion supported the observation that hybrid fishes had higher muscle protein and fat contents than their parent species (Figure S2 in Supporting Information).

The molecular mechanism of *mstnb* was studied by detecting the transcription levels of myogenesis-, protein metabolism-, and lipid metabolism-related genes in *mstnb*-deficient RCC, WR, WR-II, WR-III, RCC, and WCC. Myogenesis-related genes (*myod*, *myog*, and *myf5*) were significantly increased in *mstnb*-deficient RCC compared with wild-type RCC (Figure 7A), whereas only *myog* was significantly increased in hybrid fishes compared with RCC and WCC (Figure 8). This finding might reveal a difference between *mstnb*-deficient RCC and hybrid fishes: *mstnb*-deficient RCC exhibit muscle hypertrophy and muscle hyperplasia, whereas hybrid fishes show only muscle hypertrophy. These results indicated that *myog* plays critical roles in hypertrophy during postnatal myogenesis, which was consistent with the results from previous studies in medaka (Chisada et al., 2011). The expression levels of genes related to protein and lipid metabolism, particularly genes related to protein synthesis and adipogenesis, were significantly increased in *mstnb*-deficient RCC (Figure 7B and C). For example, the mRNA levels of *pi3k* and *akt* (protein synthesis-related genes) were increased 2.7-fold in *mstnb*-deficient RCC compared with wild-type RCC, and the mRNA level of *mtor* was also increased in *mstnb*-deficient RCC, which indicates that *mstnb* regulates protein synthesis through the PI3K-AKT-mTOR pathway in RCC. This result was consistent with previous findings obtained in mammals (Schiaffino et al., 2013). The mRNA levels of *pparγ* and *fabp3* (adipogenesis-related genes) were increased 2.1-fold in *mstnb*-deficient RCC compared with wild-type RCC. These results indicated that the absence of *mstnb* activated protein and fat synthesis and degradation pathways, and the synthesis pathway was more active than the degradation pathway, resulting in significant increases in the protein and fat contents. Furthermore, the expression levels of most protein and lipid metabolism-related genes, including *pi3k*, *akt*, *mtor*, *pparγ*, and *fabp3*, were also significantly increased in hybrid fishes compared with RCC and WCC (Figure 8). Therefore, we hypothesize that *mstnb* mainly regulates somatic growth by regulating genes related to myogenesis, protein synthesis, and adipogenesis in hybrid fishes and RCC (Figure 9).

In summary, based on our previous studies showing that hybrid fishes are characterized by rapid growth, we found that hybrid fishes were hypertrophic compared with their parent species and obtained candidate genes (*mstnb*, etc.) for rapid growth (hypertrophy) through muscle transcriptome analysis. An *mstnb*-deficient RCC line was then produced using CRISPR-Cas9, and the resulting *mstnb*-deficient RCC showed the characteristics of rapid growth, muscle hypertrophy, muscle hyperplasia, and higher protein and fat contents. Additionally, the transcription levels of myogenesis-, protein synthesis-, and adipogenesis-related genes were significantly upregulated in *mstnb*-deficient RCC, WR, WR-II, and WR-III. Our study demonstrated the key role of *mstnb* in the somatic growth of fishes derived from distant hybridization, and *mstnb*-deficient RCC could have important economic application value in aquaculture. In this study, we demonstrated the function of *mstnb* in the rapid growth of hybrid fishes, but many other genes (*fgf21*, *igf1r*, *htra1*, *igfbp7*, etc.) (Table 1) might be involved in the rapid growth of hybrid fishes. In the future, we will continue to study the mechanism of rapid growth in hybrid fishes.

MATERIALS AND METHODS

Ethics statement

The animal care and experimental protocols were certified by a professional training course for laboratory animal practitioners held by the Institute of Experimental Animals, Hunan Province, China. All efforts were made to reduce the suffering of the animals.

Body weight and muscle fiber analyses

The fishes used in this study were cultured at the Engineering Research Center of Polyploid Fish Breeding and Reproduction of the State Education Ministry, China, located at Hunan Normal University. The breeding strategies used to generate the hybrid fishes are shown in Figure S1 in Supporting Information. Two comparisons were included in this study: one comparison was between hybrid fishes (WR, WR-II, and WR-III) and their parent species (RCC and WCC), and the other comparison was between *mstnb*-deficient RCC and their wild-type siblings (RCC). The two groups were farmed in different years. Each group was cultured for 1 year under the same conditions (from fry to adult fish); 450 fish from each group (WR, WR-II, WR-III, RCC, and WCC) were cultured separately in a 150 m^2 pond, and 200 *mstnb*-deficient RCC and 200 RCC were separately cultured in a 40 m^2 pond. Fifty fish of each species were selected for body weight measurements. Furthermore, 5 fish of each species were selected for the analysis of muscle fiber. The dorsal muscle was fixed in 4% paraformaldehyde for 24 h, dehydrated through different gradients of ethanol and embedded in paraffin. Cross-sections with a thickness of 5 μm were stained with hematoxylin and eosin (H&E) and observed under a Leica inverted CW4000 microscope and a Leica LCS SP2 confocal imaging system (Leica, Germany). The outlines of individual muscle fibers, the number of fibers, and the fiber area were determined with ImageJ. Statistical data were obtained from twenty cross-sections of each fish species.

https://doi.org/10.1007/s11427-023-2487-8

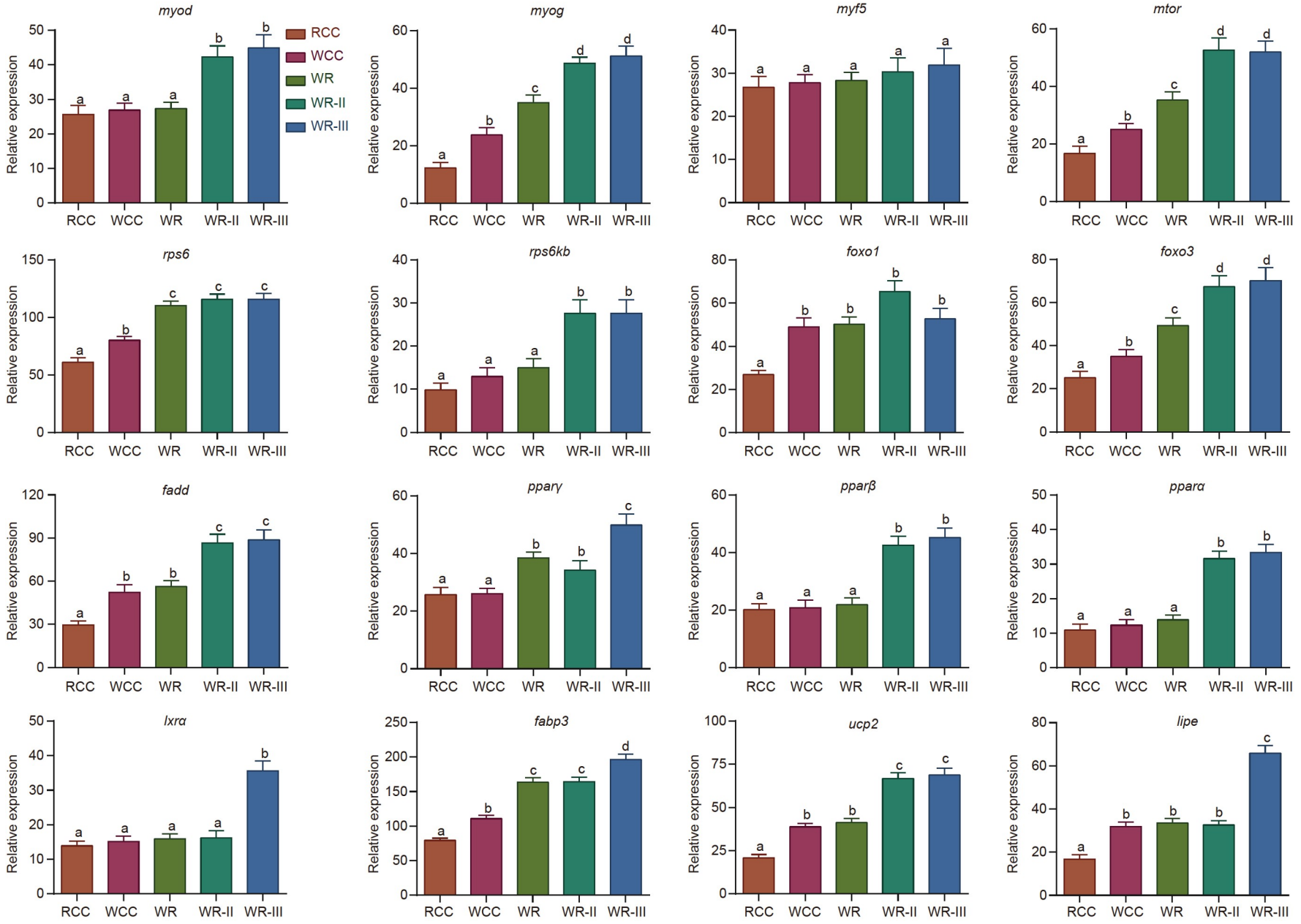

Figure 8. The relative mRNA levels of key myogenesis-, protein metabolism-, lipid metabolism-, and growth-related genes in RCC, WCC, WR, WR-II, and WR-III were determined by RT-qPCR. Different lowercase letters indicate significant differences ($P<0.05$).

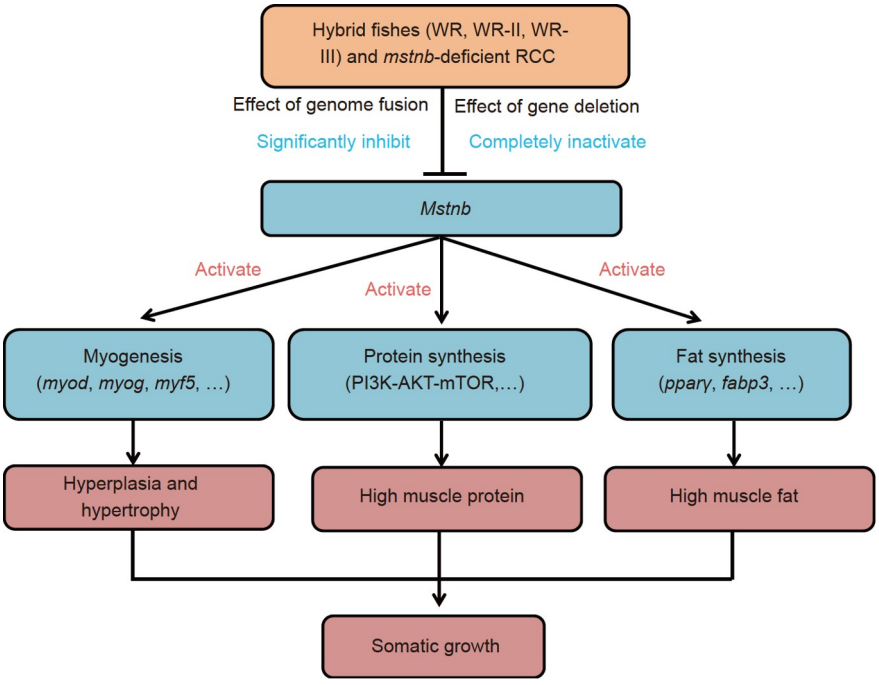

Figure 9. Model summarizing the inhibitory roles of *mstnb* during somatic growth in hybrid fishes and RCC. The genomic fusion effect of distant hybridization and the effect of gene knockout significantly reduce or completely inactivate the expression of *mstnb*. Inhibition of *mstnb* function can activate the expression of genes related to myogenesis, protein synthesis, and fat synthesis. Therefore, *mstnb* inhibition can promote muscle hypertrophy, muscle hyperplasia, and muscle protein and fat accumulation, which ultimately leads to rapid somatic growth in hybrid fishes and RCC.

Identification of candidate genes for rapid growth by transcriptome analysis

We randomly selected 3 fish each from the WR, WR-II, WR-III, and RCC for transcriptome analysis (a total of 12 samples). High-quality total RNA from the dorsal muscle was obtained using a tissue RNA kit (Omega, USA). RNA was used to construct the sequencing libraries and sequencing. After obtaining clean reads, the RCC genome was used as a reference genome for comparative analysis. We then used the DESeq2R package to identify DEGs with padj<0.01 and $|\log_2 \text{foldchange}|>2$ from the WR *vs.* RCC, WR-II *vs.* RCC, and WR-III *vs.* RCC comparisons. Based on the DEGs, growth-related genes were identified by GO functional classification and KEGG pathway analysis. We selected the growth-related DEGs shared by those obtained from the comparisons of WR, WR-II, and WR-III with RCC as candidate genes for rapid growth. The detailed methods used in the transcriptome analysis were described previously (He et al., 2023).

CDS cloning and sequencing of *mstnb* of WR, WR-II, WR-III, and WCC

The primers (Table S5 in Supporting Information) were designed based on the *mstnb* sequence of RCC (NCBI accession number: KC851952.1), and the full-length *mstnb* CDSs of WR, WR-II, WR-III, and WCC were cloned by PCR. The template cDNA was obtained by reverse transcription of RNA from muscle tissue. After gel electrophoresis and purification, the PCR products were ligated into the pMD18-T vector and transferred into *E. coli* DH5α. The positive clones were selected for sequencing, and the sequences of RCC, WR, WR-II, WR-III, WCC, and zebrafish (NCBI accession number: NM_131019.5) were aligned using BioEdit.

mstnb depletion in RCC using CRISPR-Cas9

Based on the full-length *mstnb* CDS of RCC, we used CRISPR-Cas9 to obtain the *mstnb*-deficient mutant RCC line. The guide RNA (gRNA) was designed for the CDS (*mstnb*-gRNA: GGATCGTAA-GAGCGCAGCTG) (Figure 4A) according to previously reported principles (Liu et al., 2019b), and the *mstnb*-gRNA was BLAST searched against the RCC genome to minimize off-target effects. The template for gRNA transcription *in vitro* was obtained by PCR (the primers are listed in Table S5 in Supporting Information). Cas9 mRNA and gRNA were synthesized as described previously (Liu et al., 2019b). The purified Cas9 mRNA and gRNA were mixed (Cas9 mRNA 300 ng μL^{-1}, gRNA 100 ng μL^{-1}), and the mixture was injected into the fertilized egg at the one-cell stage (approximately 15 min after fertilization at 25°C) using TransferMan NI2 (Eppendorf, Hamburg, Germany). Genomic DNA was obtained from F_0 embryos, and the target region was amplified by PCR to confirm the mutation (the primers are listed in Table S5 in Supporting Information). After F_0 reached sexual maturity, they were mated with wild-type RCC, and F_1 heterozygotes were obtained and confirmed by PCR sequencing. F_2 homozygotes were obtained by the self-crossing of F_1, and the genotypes were confirmed by PCR. The *mstnb*-deficient mutant line was obtained by self-crossing the F_2 homozygote.

Muscle nutrient analysis

The muscle nutrient profiles (protein, fat, amino acids, moisture, and ash) of one-year-old *mstnb*-deficient RCC and wild-type RCC were detected, and the protein and fat contents of one-year-old WR, WR-II, WR-III, RCC, and WCC were determined. The two groups of fish were farmed in different years. The protein content

https://doi.org/10.1007/s11427-023-2487-8

of freeze-dried muscle was measured using a fixed nitrogen distillation unit and Kjeldahl azotometer. The fat content of freeze-dried muscle was measured with a Soxhlet extractor using anhydrous ether as an extraction agent. The moisture content was measured by the vacuum freeze-drying method. The ash content was measured by combustion in a muffle furnace at 550°C. The protein was hydrolyzed to free amino acids by hydrochloric acid, and amino acid contents were measured using an Agilent 1200 series high-performance liquid chromatograph (Agilent Technologies, USA).

Western blotting

The dorsal muscle of one-year-old *mstnb*-deficient RCC and wild-type RCC was used for protein extraction. A total protein extraction kit (Sangon Biotech, Wuhan, China) was used to obtain muscle protein. The protein was isolated by sodium dodecyl sulfate-polyacrylamide gel electrophoresis (SDS-PAGE) and transferred onto polyvinylidene fluoride (PVDF) membranes (Millipore, USA). The PVDF membranes were then separately incubated with MSTN rabbit antibody (1:500, ABclonal, USA) and rabbit-anti-actin antibody (1:4,000; Sigma-Aldrich, USA). Goat-anti-rabbit IgG (1:30,000; Sigma-Aldrich) was used as the secondary antibody. The target proteins were visualized with a BCIP/NBT Alkaline Phosphatase Color Development Kit (Sigma-Aldrich). Three biological replicates were tested in this experiment.

Real-time quantitative PCR

For use in real-time quantitative PCR (qPCR), total RNA was extracted from muscle as described previously (Liu et al., 2019b). Total RNA was reverse-transcribed into cDNA using a High Capacity cDNA Reverse Transcription Kit (Thermo Fisher Scientific, USA). RT-qPCR was performed using Quant Studio 5 (Life Technologies, USA). The amplification system and reaction procedure were the same as previously reported, and three biological replicates were analyzed. All results were normalized to the expression level of the housekeeping gene β-actin and were determined as relative expression levels calculated using the $2^{-\Delta\Delta Ct}$ method. The expression levels of genes in hybrid fishes represent as the total expression for homeolog pair. The primers used for RT-qPCR are listed in Table S5 in Supporting Information.

Statistical analysis

Statistical analysis was performed using unpaired, two-tailed Student's *t*-test or one-way analysis of variance (ANOVA) with the post hoc least significant difference (LSD) method. SPSS 16.0 software was used for data analysis, and $P<0.05$ was regarded to indicate statistical significance.

Data availability statement

The complete clean reads for these libraries have been uploaded to the NCBI Sequence Read Archive site (http://www.ncbi.nlm.nih.gov/sra/; Accession Nos. SRR25395549, SRR25395550, SRR25395551, SRR25395552, SRR25395553, SRR25395554, SRR25395555, SRR25395556, SRR25395557, SRR25395558, SRR25395559, and SRR25395560).

Compliance and ethics

The author(s) declare that they have no conflict of interest.

Acknowledgement

This work was supported by the National Natural Science Foundation of China (32002382, 32293252, U19A2040, 32293254), the National Key Research and Development Program of China (2023YFD2400202), the Natural Science Foundation of Hunan Province (2021JJ40339), the Training Program for Excellent Young Innovators of Changsha (kq2209013), the Earmarked Fund for Agriculture Research System of China (CARS-45), the Laboratory of Lingnan Modern Agriculture Project (NT2021008), the 111 Project (D20007), and Special Science Found of Nansha-South China Agricultural University Fishery Research Institute, Guangzhou.

Supporting information

The supporting information is available online at https://doi.org/10.1007/s11427-023-2487-8. The supporting materials are published as submitted, without typesetting or editing. The responsibility for scientific accuracy and content remains entirely with the authors.

References

Argue, B.J., Kuhlers, D.L., Liu, Z., and Dunham, R.A. (2014). Growth of channel catfish (*Ictalurus punctatus*), blue catfish (*I. furcatus*), and their F_1, F_2, F_3, and F_1 reciprocal backcross hybrids in earthen ponds. J Anim Sci 92, 4297–4305.

Bartley, D.M., Rana, K., and Immink, A.J. (2000). The use of interspecific hybrids in aquaculture and fisheries. reviews in fish. Rev Fish Biol Fish 10, 325–337.

Berry, C., Thomas, M., Langley, B., Sharma, M., and Kambadur, R. (2002). Single cysteine to tyrosine transition inactivates the growth inhibitory function of Piedmontese myostatin. Am J Physiol Cell Physiol 283, C135–C141.

Beyer, T.A., Narimatsu, M., Weiss, A., David, L., and Wrana, J.L. (2013). The TGFβ superfamily in stem cell biology and early mammalian embryonic development. Biochim Biophys Acta Gen Subj 1830, 2268–2279.

Chisada, S., Okamoto, H., Taniguchi, Y., Kimori, Y., Toyoda, A., Sakaki, Y., Takeda, S., and Yoshiura, Y. (2011). Myostatin-deficient medaka exhibit a double-muscling phenotype with hyperplasia and hypertrophy, which occur sequentially during post-hatch development. Dev Biol 359, 82–94.

Crispo, M., Mulet, A., Tesson, L., Barrera, N., Cuadro, F., dos Santos-Neto, P., Nguyen, T., Crénéguy, A., Brusselle, L., and Anegón, I. (2015). Efficient generation of myostatin knock-out sheep using CRISPR/Cas9 technology and microinjection into zygotes. PLoS ONE 10, e0136690.

Deng, B., Zhang, F., Wen, J., Ye, S., Wang, L., Yang, Y., Gong, P., and Jiang, S. (2017). The function of myostatin in the regulation of fat mass in mammals. Nutr Metab (Lond) 14, 29.

Gao, Y., Dai, Z., Shi, C., Zhai, G., Jin, X., He, J., Lou, Q., and Yin, Z. (2016). Depletion of myostatin b promotes somatic growth and lipid metabolism in zebrafish. Front Endocrinol 7, 88.

Gaylord, T.G., and Gatlin III, D.M. (2000). Dietary lipid level but not l-carnitine affects growth performance of hybrid striped bass (*Morone chrysops* ♀×*M. saxatilis* ♂). Aquaculture 190, 237–246.

Gong, D., Tao, M., Xu, L., Hu, F., Wei, Z., Wang, S., Wang, Y., Liu, Q., Wu, C., Luo, K., et al. (2022). An improved hybrid bream derived from a hybrid lineage of *Megalobrama amblycephala* (♀)×*Culter alburnus* (♂). Sci China Life Sci 65, 1213–1221.

Guo, R., Wan, Y., Xu, D., Cui, L., Deng, M., Zhang, G., Jia, R., Zhou, W., Wang, Z., Deng, K., et al. (2016). Generation and evaluation of myostatin knock-out rabbits and goats using CRISPR/Cas9 system. Sci Rep 6, 29855.

He, J., Zhao, F., Chen, B., Cui, N., Li, Z., Qin, J., Luo, L., Zhao, C., and Li, L. (2023). Alterations in immune cell heterogeneities in the brain of aged zebrafish using single-cell resolution. Sci China Life Sci 66, 1358–1378.

Hu, F., Zhong, H., Wu, C., Wang, S., Guo, Z., Tao, M., Zhang, C., Gong, D., Gao, X., Tang, C., et al. (2021). Development of fisheries in China. Reprod Breed 1, 64–79.

Johnston, I.A. (2006). Environment and plasticity of myogenesis in teleost fish. J Exp Biol 209, 2249–2264.

Kambadur, R., Sharma, M., Smith, T.P.L., and Bass, J.J. (1997). Mutations in *myostatin* (*GDF8*) in double-muscled Belgian Blue and piedmontese cattle. Genome Res 7, 910–915.

Kerr, T., Roalson, E.H., and Rodgers, B.D. (2005). Phylogenetic analysis of the myostatin gene sub-family and the differential expression of a novel member in zebrafish. Evol Dev 7, 390–400.

Khalil, K., Elayat, M., Khalifa, E., Daghash, S., Elaswad, A., Miller, M., Abdelrahman, H., Ye, Z., Odin, R., Drescher, D., et al. (2017). Generation of myostatin gene-edited channel catfish (*Ictalurus punctatus*) via zygote injection of CRISPR/Cas9 system. Sci Rep 7, 7301.

Kishimoto, K., Washio, Y., Yoshiura, Y., Toyoda, A., Ueno, T., Fukuyama, H., Kato, K., and Kinoshita, M. (2018). Production of a breed of red sea bream Pagrus major with an increase of skeletal muscle mass and reduced body length by genome editing with CRISPR/Cas9. Aquaculture 495, 415–427.

Lee, S.J., Huynh, T.V., Lee, Y.S., Sebald, S.M., Wilcox-Adelman, S.A., Iwamori, N., Lepper, C., Matzuk, M.M., and Fan, C.M. (2012). Role of satellite cells versus myofibers in muscle hypertrophy induced by inhibition of the myostatin/activin

signaling pathway. Proc Natl Acad Sci USA 109, E2353–E2360.
Lee, S.J., Lehar, A., Liu, Y., Ly, C.H., Pham, Q.M., Michaud, M., Rydzik, R., Youngstrom, D.W., Shen, M.M., Kaartinen, V., et al. (2020). Functional redundancy of type I and type II receptors in the regulation of skeletal muscle growth by myostatin and activin A. Proc Natl Acad Sci USA 117, 30907–30917.
Li, J., Yang, C., Huang, L., Zeng, K., Cao, X., and Gao, J. (2019). Inefficient ATP synthesis by inhibiting mitochondrial respiration causes lipids to decrease in MSTN-lacking muscles of loach *Misgurnus anguillicaudatus*. Funct Integr Genomics 19, 889–900.
Li, W., Liu, J., Tan, H., Luo, L., Cui, J., Hu, J., Wang, S., Liu, Q., Hu, F., Tang, C., et al. (2018). Asymmetric expression patterns reveal a strong maternal effect and dosage compensation in polyploid hybrid fish. BMC Genomics 19, 517.
Li, X.Y., Mei, J., Ge, C.T., Liu, X.L., and Gui, J.F. (2022). Sex determination mechanisms and sex control approaches in aquaculture animals. Sci China Life Sci 65, 1091–1122.
Liu, Q., Liu, J., Liang, Q., Qi, Y., Tao, M., Zhang, C., Qin, Q., Zhao, R., Chen, B., and Liu, S. (2019a). A hybrid lineage derived from hybridization of *Carassius cuvieri* and *Carassius auratus* red var. and a new type of improved fish obtained by back-crossing. Aquaculture 505, 173–182.
Liu, Q., Liu, J., Yuan, L., Li, L., Tao, M., Zhang, C., Qin, Q., Chen, B., Ma, M., Tang, C., et al. (2020). The establishment of the fertile fish lineages derived from distant hybridization by overcoming the reproductive barriers. Reproduction 159, R237–R249.
Liu, Q., Luo, K., Zhang, X., Liu, F., Qin, Q., Tao, M., Wen, M., Tang, C., and Liu, S. (2021a). A new type of triploid fish derived from the diploid hybrid *crucian carp* (♀) × autotetraploid fish (♂). Reprod Breed 1, 122–127.
Liu, Q., Qi, Y., Liang, Q., Song, J., Liu, J., Li, W., Shu, Y., Tao, M., Zhang, C., Qin, Q., et al. (2019b). Targeted disruption of tyrosinase causes melanin reduction in *Carassius auratus cuvieri* and its hybrid progeny. Sci China Life Sci 62, 1194–1202.
Liu, Q., Qi, Y., Liang, Q., Xu, X., Hu, F., Wang, J., Xiao, J., Wang, S., Li, W., Tao, M., et al. (2018). The chimeric genes in the hybrid lineage of *Carassius auratus cuvieri* (♀)×*Carassius auratus* red var. (♂). Sci China Life Sci 61, 1079–1089.
Liu, Q., Zhang, X., Liu, J., Liu, F., Shi, F., Qin, Q., Tao, M., Tang, C., and Liu, S. (2021b). A new type of allodiploid hybrids derived from female *Megalobrama amblycephala* × male *Gobiocypris rarus*. Front Genet 12, 685914.
Liu, S.J. (2010). Distant hybridization leads to different ploidy fishes. Sci China Life Sci 53, 416–425.
Liu, S., Luo, J., Chai, J., Ren, L., Zhou, Y., Huang, F., Liu, X., Chen, Y., Zhang, C., Tao, M., et al. (2016). Genomic incompatibilities in the diploid and tetraploid offspring of the goldfish × common carp cross. Proc Natl Acad Sci USA 113, 1327–1332.
Liu, S., Wang, S., Liu, Q., Zhou, Y., Zhang, C., Tao, M., and Luo, K. (2022). The summary of fish distant hybridization. In: Liu, S, ed. Fish Distant Hybridization. Singapore: Springer. 325–343.
McPherron, A.C., and Lee, S.J. (1997). Double muscling in cattle due to mutations in the myostatin gene. Proc Natl Acad Sci USA 94, 12457–12461.
McPherron, A.C., and Lee, S.J. (2002). Suppression of body fat accumulation in myostatin-deficient mice. J Clin Invest 109, 595–601.
Ou, M., Mao, H., Luo, Q., Zhao, J., Liu, H., Zhu, X., Chen, K., and Xu, H. (2019). The DNA methylation level is associated with the superior growth of the hybrid fry in snakehead fish (*Channa argus* × *Channa maculata*). Gene 703, 125–133.
Ren, L., Li, W., Qin, Q., Dai, H., Han, F., Xiao, J., Gao, X., Cui, J., Wu, C., Yan, X., et al. (2019). The subgenomes show asymmetric expression of alleles in hybrid lineages of *Megalobrama amblycephala*×*Culter alburnus*. Genome Res 29, 1805–1815.
Ren, L., Zhang, H., Luo, M., Gao, X., Cui, J., Zhang, X., and Liu, S. (2022). Heterosis of growth trait regulated by DNA methylation and miRNA in allotriploid fish. Epigenet Chromatin 15, 19.
Rescan, P.Y. (2005). Muscle growth patterns and regulation during fish ontogeny. Gen Comp Endocrinol 142, 111–116.
Rescan, P.Y. (2008). New insights into skeletal muscle development and growth in teleost fishes. J Exp Zool Pt B 310B, 541–548.
Sartori, R., Romanello, V., and Sandri, M. (2021). Mechanisms of muscle atrophy and hypertrophy: implications in health and disease. Nat Commun 12, 330.
Schiaffino, S., Dyar, K.A., Ciciliot, S., Blaauw, B., and Sandri, M. (2013). Mechanisms regulating skeletal muscle growth and atrophy. FEBS J 280, 4294–4314.
Shan, T., Liang, X., Bi, P., and Kuang, S. (2013). Myostatin knockout drives browning of white adipose tissue through activating the AMPK-PGC1α-Fndc5 pathway in muscle. FASEB J 27, 1981–1989.
Shi, C., Lou, Q., Fu, B., Jin, J., Huang, J., Lu, Y., Jin, X., He, J., Zhai, G., Xie, S., et al. (2022). Genomic polymorphisms at the crhr2 locus improve feed conversion efficiency through alleviation of hypothalamus-pituitary-interrenal axis activity in gibel carp (*Carassius gibelio*). Sci China Life Sci 65, 206–214.
Tao, B., Tan, J., Chen, L., Xu, Y., Liao, X., Li, Y., Chen, J., Song, Y., and Hu, W. (2021). CRISPR/Cas9 system-based myostatin-targeted disruption promotes somatic growth and adipogenesis in loach, *Misgurnus anguillicaudatus*. Aquaculture 544, 737097.
Taylor, W.E., Bhasin, S., Artaza, J., Byhower, F., Azam, M., Willard Jr., D.H., Kull Jr., F.C., and Gonzalez-Cadavid, N. (2001). Myostatin inhibits cell proliferation and protein synthesis in C_2 C_{12} muscle cells. Am J Physiol Endocrinol Metab 280, E221–E228.
Thomas, M., Langley, B., Berry, C., Sharma, M., Kirk, S., Bass, J., and Kambadur, R. (2000). Myostatin, a negative regulator of muscle growth, functions by inhibiting myoblast proliferation. J Biol Chem 275, 40235–40243.
Wang, J., Xiao, J., Zeng, M., Xu, K., Tao, M., Zhang, C., Duan, W., Liu, W.B., Luo, K.K., Liu, Y., et al. (2015a). Genomic variation in the hybrids of white crucian carp and red crucian carp: evidence from ribosomal DNA. Sci China Life Sci 58, 590–601.
Wang, K., Ouyang, H., Xie, Z., Yao, C., Guo, N., Li, M., Jiao, H., and Pang, D. (2015b). Efficient generation of myostatin mutations in pigs using the CRISPR/Cas9 system. Sci Rep 5, 16623.
Wang, Y., Liu, Y.J., Tian, L.X., Du, Z.Y., Wang, J.T., Wang, S., and Xiao, W.P. (2005). Effects of dietary carbohydrate level on growth and body composition of juvenile tilapia, *Oreochromis niloticus*×*O. aureus*. Aquac Res 36, 1408–1413.
Whittemore, L.A., Song, K., Li, X., Aghajanian, J., Davies, M., Girgenrath, S., Hill, J.J., Jalenak, M., Kelley, P., Knight, A., et al. (2003). Inhibition of myostatin in adult mice increases skeletal muscle mass and strength. Biochem Biophys Res Commun 300, 965–971.
Wu, Y., Wu, T., Yang, L., Su, Y., Zhao, C., Li, L., Cai, J., Dai, X., Wang, D., and Zhou, L. (2023). Generation of fast growth Nile tilapia (*Oreochromis niloticus*) by myostatin gene mutation. Aquaculture 562, 738762.
Xiao, H., Xu, Z., Zhu, X., Wang, J., Zheng, Q., Zhang, Q., Xu, C., Tao, W., and Wang, D. (2022). Cortisol safeguards oogenesis by promoting follicular cell survival. Sci China Life Sci 65, 1563–1577.
Xie, S., Niu, D., Wei, K., Dong, Z., and Li, J. (2018). Polymorphisms in the *FOXO* gene are associated with growth traits in the Sanmen breeding population of the razor clam *Sinonovacula constricta*. Aquac Fish 3, 177–183.
Xu, C., Wu, G., Zohar, Y., and Du, S.J. (2003). Analysis of *myostatin* gene structure, expression and function in zebrafish. J Exp Biol 206, 4067–4079.
Yeh, Y.C., Kinoshita, M., Ng, T.H., Chang, Y.H., Maekawa, S., Chiang, Y.A., Aoki, T., and Wang, H.C. (2017). Using CRISPR/Cas9-mediated gene editing to further explore growth and trade-off effects in myostatin-mutated F4 medaka (*Oryzias latipes*). Sci Rep 7, 11435.
Yu, B., Lu, R., Yuan, Y., Zhang, T., Song, S., Qi, Z., Shao, B., Zhu, M., Mi, F., and Cheng, Y. (2016). Efficient TALEN-mediated myostatin gene editing in goats. BMC Dev Biol 16, 26.
Yu, P., Wang, Y., Li, Z., Jin, H., Li, L.L., Han, X., Wang, Z.W., Yang, X.L., Li, X.Y., Zhang, X.J., et al. (2022). Causal gene identification and desirable trait recreation in goldfish. Sci China Life Sci 65, 2341–2353.
Zhong, Z., Niu, P., Wang, M., Huang, G., Xu, S., Sun, Y., Xu, X., Hou, Y., Sun, X., Yan, Y., et al. (2016). Targeted disruption of sp7 and myostatin with CRISPR-Cas9 results in severe bone defects and more muscular cells in common carp. Sci Rep 6, 22953.

https://doi.org/10.1007/s11427-023-2487-8